JOC The Journal of Organic Chemistry

Article

pubs.acs.org/joc

Photodeamination Reaction Mechanism in Aminomethyl *p*-Cresol Derivatives: Different Reactivity of Amines and Ammonium Salts

Đani Škalamera,[†] Cornelia Bohne,[‡] Stephan Landgraf,[§] and Nikola Basarić*,[†]

[†]Department of Organic Chemistry and Biochemistry, Ruđer Bošković Institute, Bijenička cesta 54, 10 000 Zagreb, Croatia

[‡]Department of Chemistry, University of Victoria, Box 3065 STN CSC, Victoria, BC V8W 3 V6, Canada

[§]Institute of Physical and Theoretical Chemistry, Graz University of Technology, Stremayrgasse 9, A-8010 Graz, Austria

Supporting Information

ABSTRACT: Derivatives of *p*-cresol **1**−**4** were synthesized, and their photochemical reactivity, acid−base, and photophysical properties were investigated. The photoreactivity of amines **1** and **3** is different from that for the corresponding ammonium salts **2** and **4**. All compounds have low fluorescence quantum yields because the excited states undergo deamination reactions, and for all cresols the formation of quinone methides (QMs) was observed by laser flash photolysis. The reactivity observed is a consequence of the higher acidity of the S_1 states of these *p*-cresols and the ability for excited-state intramolecular proton transfer (ESIPT) to occur in the case of **1** and **3**, but not for salts **2** and **4**. In aqueous solvent, deamination depends largely on the prototropic form of the molecule. The most efficient deamination takes place when monoamine is in the zwitterionic form (pH 9−11) or diamine is in the monocationic form (pH 7−9). **QM1**, **QM3**, and **QM4** react with nucleophiles, and **QM1** exhibits a shorter lifetime when formed from **1** (τ in CH_3CN = 5 ms) than from **2** (τ in CH_3CN = 200 ms) due to the reaction with eliminated dimethylamine, which acts as a nucleophile in the case of **QM1**. Bifunctional **QM4** undergoes two types of reactions with nucleophiles, giving adducts or new QM species. The mechanistic diversity uncovered is of significance to biological systems, such as for the use of bifunctional QMs to achieve DNA cross-linking.

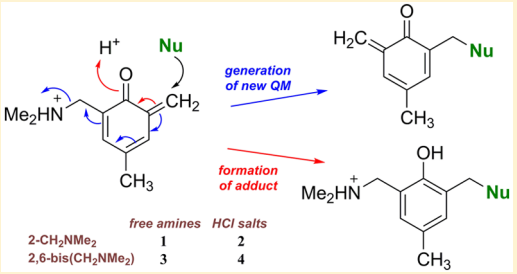

INTRODUCTION

Quinone methides (QMs) are reactive intermediates encountered in the chemistry and photochemistry of phenols.[1] QMs have biological activity,[2−6] and they have been shown to react with amino acids,[7,8] proteins,[9] nucleobases,[10−12] and DNA.[13−16] Some antineoplastic antibiotics such as mitomycin exhibit antiproliferative action on metabolic formation of QMs and subsequent alkylation of DNA.[17−19] Moreover, we have recently demonstrated that antiproliferative activity of photogenerated QMs stems from their reaction with intracellular proteins rather than with DNA.[20]

QMs can be generated in thermal reactions including oxidation of phenols,[21] dehydration from hydroxybenzyl alcohols,[22,23] elimination of nitriles from 1,2-benzoxazines,[24] and fluoride-induced desilylation.[14,15] Photochemical methods enable access to QMs under much milder conditions and provide spatial and temporal control of the process, which is particularly appealing in biological systems.[4,5] The photochemical methods to generate QMs rely on the photoelimination of HF[25] or acetic acid,[26] photodehydration[27,28] or phototautomerization of suitably substituted phenols[29] or naphthols,[30] and photohydration of alkenes.[31] The most common photochemical method to generate QMs in biological systems is photodeamination from the Mannich salts of the corresponding phenols,[8,32] which can also be facilitated in an intramolecular photoinduced electron-transfer reaction with naphthalene diimide as photooxidizing agent.[33] Photodeamination of Mannich salts has recently been applied in the investigation of biological activity of QMs,[34,35] and the ability of naphthalenediimide QM derivatives to selectively target guanine quadruplex structures has been demonstrated.[36−38]

In spite of numerous biological implications of photodeamination, a systematic mechanistic investigation of QM formation through deamination reactions and QM reactivity is lacking. Therefore, it is of pivotal importance to investigate the mechanism of QM formation in deamination as well as reactivity of the corresponding QMs. Herein, we report a mechanistic study of the photodeamination for a series of four cresol derivatives **1**−**4**. The molecules were designed to probe for the effect of the nitrogen protonation (**1** and **3** vs salts **2** and **4**) and to determine the differences between mono- and disubstitution (**1** and **2** vs **3** and **4**) on the efficiency of QM generation and its reactivity. Bifunctional **3** and **4** are potentially applicable for DNA cross-linking, and it is important to understand the difference in reactivity compared to **1** and **2**. The photochemical reactivity of **1**−**4** was investigated by preparative irradiations and compared to the reactivity of ether **5** that cannot give QM. Photophysical properties were investigated by fluorescence spectroscopy, whereas formation of the QMs and other potential reactive intermediates was probed by laser flash photolysis (LFP).

Received: August 26, 2015
Published: October 13, 2015

DOI: 10.1021/acs.joc.5b01991
J. Org. Chem. 2015, 80, 10817−10828

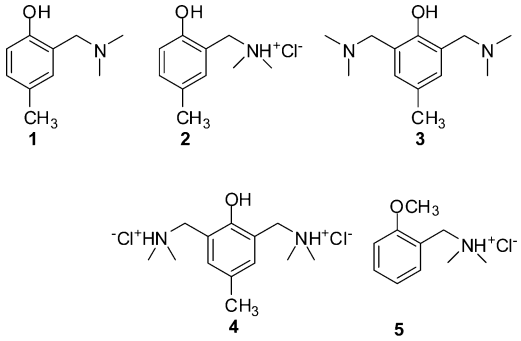

RESULTS

Synthesis. Cresol derivatives **1**−**4** were prepared in high yields (87−93%) by a simple procedure from *p*-cresol and Eschenmoser's salt, which was used in equimolar ratio to form **1** or prepared in excess in situ to yield **3** (Scheme 1). *p*-Cresol was chosen as a substrate in the Mannich reaction so that the methyl group prevented the reaction at the *para*-position, yielding only **1** or **3**, and facilitated the purification. The free bases were transformed to the corresponding salts **2** and **4** in ethereal HCl solutions.

Ether **5**[39] was prepared in excellent yield from salicylaldehyde (Scheme 2), which was methylated to **6**.[40] A reaction of **6** with dimethylamine, and subsequent hydrogenation of imine on PtO_2, furnished **7**, which was transformed into salt **5**.

UV−vis and Fluorescence Measurements. Compounds **1**−**4** were characterized in different solvents by absorption and fluorescence spectroscopy (Figure 1 and Figures S1−S12 in the Supporting Information). Absorption spectra are about 10 nm bathochromically shifted compared to the phenol $S_0 \rightarrow S_1$ absorption.[41] Fluorescence spectra taken in CH_3CN are structureless with one emission band for **2** and **4** and dual emission for **1** and **3** (Figure 1). The emission at 308−318 nm is attributed to the fluorescence of phenol, whereas the band at 370 nm, seen only for **1** and **3**, corresponds to the emission of phenolate formed by excited-state intramolecular proton transfer (ESIPT) from acidic phenol OH to the basic dimethylamine nitrogen (Table 1). Upon electronic excitation, phenols exhibit enhanced acidity (unsubstituted phenol $pK_a^* = 3.6$).[42,43] Since the basic amine nitrogen is in close proximity to phenol OH in **1** and **3**, but not in **2** and **4** wherein the amine groups are protonated, excitation of **1** and **3** to S_1 leads to ESIPT, as demonstrated in similar precedent examples.[44−47]

Quantum yields of fluorescence for **1**−**4** were measured by use of anisole in cyclohexane ($\Phi_f = 0.29$)[48] as a reference (eq S1 , Supporting Information). Generally, all compounds are very weakly fluorescent in CH_3CN with the fluorescent quantum yields in the range 0.001−0.05, indicating efficient nonradiative deactivation from S_1 (Table 1). In addition, Φ_f is approximately 10 times lower for amines **1** and **3** when compared to **2** and **4** due to deactivation by ESIPT. We attempted to measure fluorescence decays of **1**−**4** by time-correlated single photon counting (SPC). However, due to the very weak fluorescence, multiexponential decays with contribution of short decay components (<100 ps), and high photochemical reactivity of the molecules, no reliable time-resolved data could be obtained on the setup used.

Addition of protic solvent (H_2O) to CH_3CN solutions of **1**−**4** changed their photophysical properties. When the addition of H_2O did not exceed the concentration of 2 M, the fluorescence of **2** and **4** was quenched, but increased fluorescence was observed for **1** and **3** (Figures S3, S6, S9, and S12, Supporting Information). The increase of fluorescence for **1** and **3** by addition of H_2O is due to partial blocking of the efficient

Scheme 2. Synthesis of Ether 5

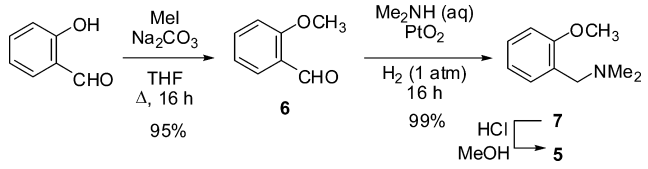

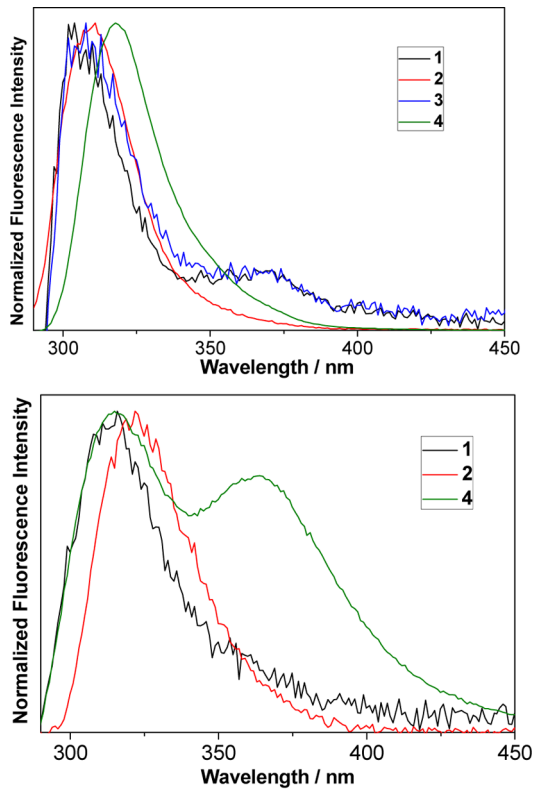

Figure 1. Normalized fluorescence spectra at the emission maxima of **1**−**4** in CH_3CN (top, λ_{ex} = 260 nm) and CH_3CN−H_2O (1:1) for **1**, **2**, and **4** (bottom, λ_{ex} = 260 nm).

Scheme 1. Preparation of 1−4

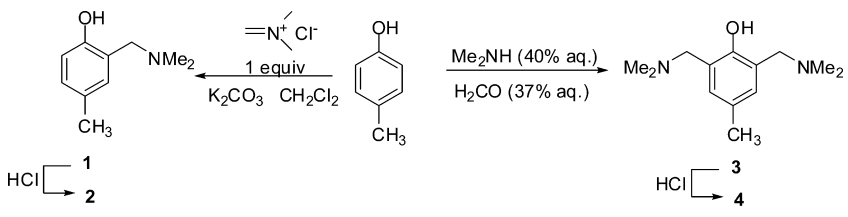

DOI: 10.1021/acs.joc.5b01991
J. Org. Chem. 2015, 80, 10817−10828

Table 1. Maximum in the Absorption and Emission Spectra (λ_{max}) and Fluorescence Quantum Yields (Φ_f) of 1–4 in Acetonitrile

	λ_{max} [a] (nm)	λ_{max} [b] (nm)	Φ_f (CH_3CN)[c]
1	283	308	$(1.5 \pm 0.5) \times 10^{-3}$
		370 (shoulder)	
2	286	310	$(12.6 \pm 0.2) \times 10^{-3}$
3	283	308	$(3 \pm 1) \times 10^{-3}$
		370 (shoulder)	
4	286	318	$(52.2 \pm 0.8) \times 10^{-3}$

[a]Maximum in the absorption spectrum. [b]Maximum in the emission spectrum (λ_{ex} = 260 nm). [c]Fluorescence quantum yields measured by use of anisole in cyclohexane as a reference (Φ_f = 0.29).[48]

nonradiative deactivation pathway from S_1 by ESIPT. Namely, addition of nonbuffered H_2O induced protonation of the basic amine nitrogens and formation of **2** and **4**, so that these molecules do not bear a basic center (Schemes 3 and 4). On

Scheme 3. Protonation Equilibria for 2

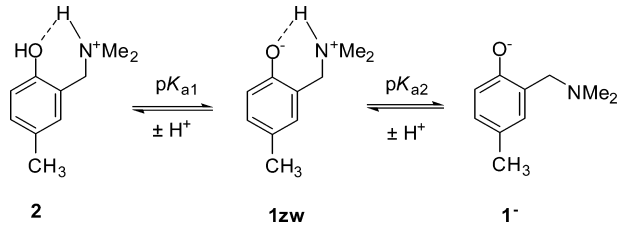

the contrary, quenching of fluorescence for **2** and **4** by addition of H_2O indicates operation of an additional nonradiative deactivation channel, presumably ESPT to solvent. CH_3CN cannot mediate deprotonation of the phenol in S_1, so presence of a protic solvent (H_2O) is required to enable ESPT.[49,50] In particular, the fluorescence spectrum for **4** in CH_3CN–H_2O exhibits a strong band at 370 nm (Figure 1 bottom) attributed to the fluorescence of phenolate (in 3^+ or **3zw**).

Acid–base Properties of 2 and 4. Acid–base properties were investigated for **2** and **4** by UV–vis pH titrations. The titrations were performed in H_2O in the absence of an ionic buffer by addition of small amounts of NaOH or HCl to adjust the pH. The spectra were processed by multivariate nonlinear regression analysis using the SPECFIT software[51–53] to reveal the pK_a values (Table 2).

The increase of pH for the aqueous solution of **2** in the range 6–10 induced significant UV–vis spectral changes (Figures S13 and S14, Supporting Information). The band at ~286 nm disappeared with concomitant formation of a new bathochromically shifted band at ~302 nm. The spectral change is in agreement with the formation of phenolate **1zw** (Scheme 3) where bathochromic shift is due to a larger stabilization of S_1

Table 2. pK_a Values for 2 and 4 at 25 °C in Aqueous Solution[a]

compd	2	4
pK_{a1}	8.46 ± 0.01	5.87 ± 0.01
pK_{a2}	11.15 ± 0.01	10.00 ± 0.02
pK_{a3}		12.31 ± 0.02

[a]The titration was conducted in aqueous solution without ionic buffer. pK_{a1} corresponds to the first equilibrium in Schemes 3 and 4, while pK_{a2} and pK_{a3} correspond to the subsequent equilibria.

than S_0 by deprotonation. The pK_a value for the equilibrium between **2** and **1zw** is lower than for the parent *p*-cresol (pK_a = 10.2)[54] owing to a stabilization of the negative charge in **1zw** by an intramolecular H bond. However, some influence on the pK_a value may be imposed by the nonconstant ionic strength of the solution at different pH values. Further increase of pH in the range 10–12 induced deprotonation of the amine moiety (see Figure S15, Supporting Information, for the distribution of species with pH). Because of the H bond between the amine NH and the phenolate O^- at the chromophore, the deprotonation resulted in the spectral changes.

The UV–vis spectra for **4** at different pH values are shown in Figure 2. The titration gave rise to three distinctive pH regions with different spectral responses. In the pH region between 3 and 8, the most pronounced spectral changes were observed due to the deprotonation of the phenolic OH. In contrast to the low acidity of phenols (pK_a = 9.89–9.91),[41] the pK_{a1} of **4** is significantly lower (Table 2) due the stabilization of phenolate in 3^+ by two intramolecular H bonds with the ammonium ion and compensation of the negative charge by two positive charges (Scheme 4). A similar influence on the acidity has been reported for phenols substituted with *o*-amide groups.[55] The second deprotonation equilibrium is observed in the pH region between 8.3 and 11 and marked by a decrease of the phenolate absorptivity at ~308 nm. The low pK_{a2} value corresponding to the first amine deprotonation is due to a high acidity of this ammonium ion owing to H bonds with phenolate in 3^+. Breaking of the H bond with the chromophore gives rise to the observed spectral changes. The pK_a for the second amine deprotonation is significantly higher. It is more difficult to remove a proton from neutral molecule **3zw** and form anion 3^- because it leads to breaking of the last intramolecular hydrogen bond (see Figure S16 , Supporting Information, for the distribution of species with pH).

Measurements to construct a Förster cycle were performed to show that S_1 of **1**–**4** exhibits enhanced acidity despite the limitations in using this method.[42] Of importance for this work is the trend in the pK_a* values and not in the absolute value obtained. The difference in the emission maxima of phenol and phenolate seen in the spectra of **4** in aqueous CH_3CN (eq S2, Supporting Information) gave a ΔpK_a of 8.2. Fluorescence titrations were performed to reveal pK_a* values, but because of

Scheme 4. Protonation Equilibria for 4

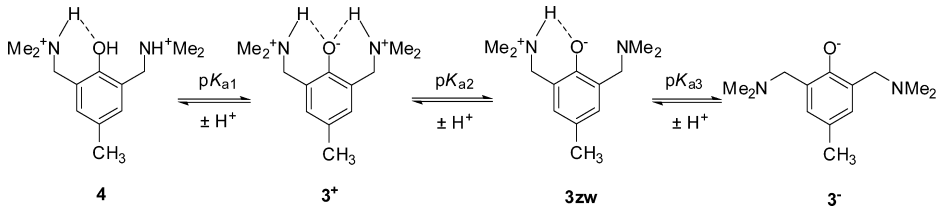

DOI: 10.1021/acs.joc.5b01991
J. Org. Chem. 2015, 80, 10817–10828

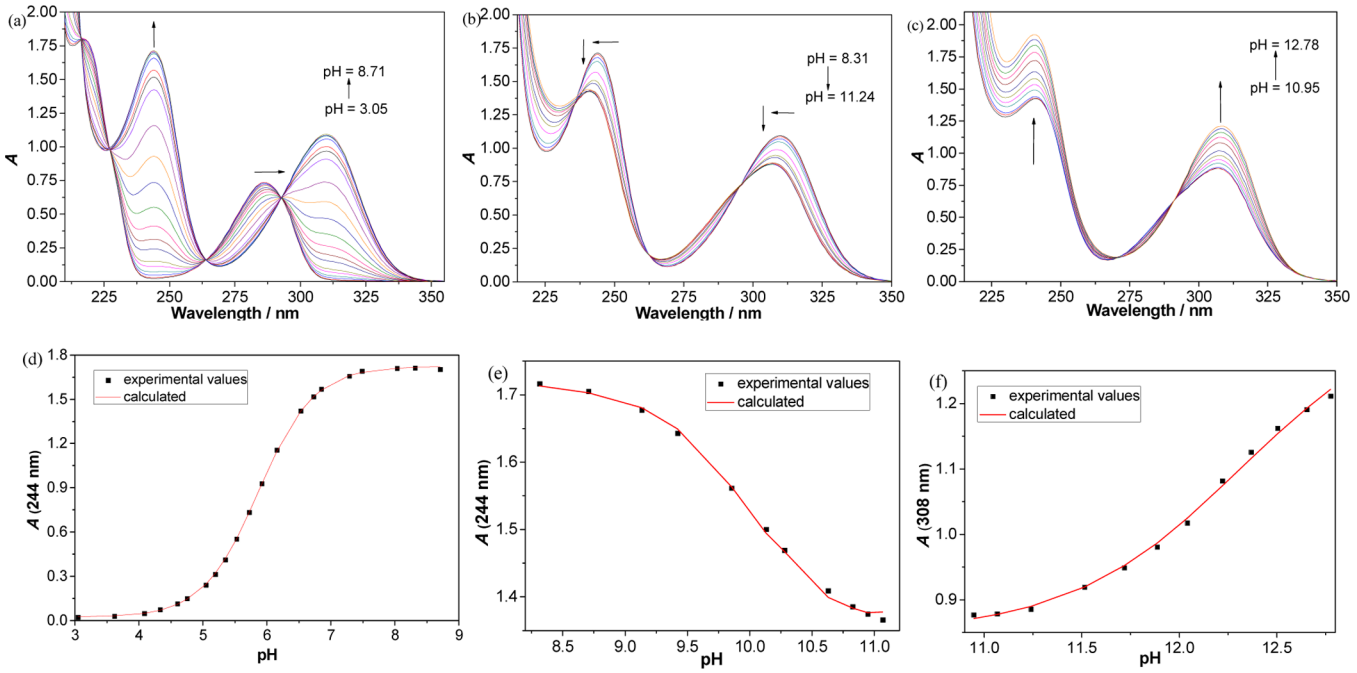

Figure 2. Absorption spectra of **4** ($c = 2.66 \times 10^{-4}$ M) in H_2O at different pH values (a) from 3.05 to 8.71, (b) from 8.31 to 11.24, and (c) from 10.95 to 12.78 and dependence of the absorbance at 244 nm (d and e) and at 308 nm (f), corresponding to a–c, respectively. The calculated values (—) were obtained by nonlinear regression analysis of the experimental values (■) using the SPECFIT software. The titration was performed at 25 °C from acidic solution (HCl) by addition of NaOH. The spectra were corrected for dilutions.

the low fluorescence intensity we were not able to process the data with satisfactory accuracy (see Figures S17 and S18). Nevertheless, the titrations indicated a decrease of pK_a values upon excitation for both **2** and **4**, in agreement with the Förster cycle analysis.

Photochemical Reactivity. Based on literature precedent,[8,56] it is expected that irradiation of **1**–**4** in CH_3OH–H_2O gives rise to photomethanolysis products via QM intermediates. Preparative irradiations of **2** and **4** were conducted by irradiating CH_3OH–H_2O (4:1) solutions at 300 nm and by analyzing the composition of the solutions by HPLC. Methanolysis of **2** run to a conversion of 80% gave methyl ether **8**[57] with a yield of 77%. An additional product, presumably alcohol **9**, was detected by HPLC but was not isolated due to the small quantities formed. Preferable formation of **8** is logical because of the better nucleophilicity of CH_3OH compared to H_2O. In addition, alcohol **9** under the same reaction conditions undergoes methanolysis and gives **8**, albeit with lower quantum efficiency (Scheme 5).[27]

Photomethanolysis of **4** conducted in CH_3OH–H_2O (4:1) to conversion of 100% gave **11** quantitatively, which was isolated and characterized by NMR. The shorter irradiation of **4** until the conversion was 50% and separation of the mixture by HPLC gave **10** (7%, isolated yield) and **11**[58] (30%, isolated yield, Scheme 6). Irradiation of **1** and **3** gave the same products as **2** and **4**, respectively.

As described above, the presence of H_2O changes the photophysical properties of **1**–**4**. Therefore, we conducted photomethanolysis of **1** and **2** in CH_3OH at different H_2O concentrations where solutions were irradiated simultaneously and the progress of the reaction was monitored by HPLC (Figures S19–S20, Supporting Information). The solutions compared had the same concentrations of compound, and the absorbance at the excitation wavelength was above 2, ensuring that all photons were absorbed. Addition of H_2O did not affect

Scheme 5. Photomethanolysis of 2

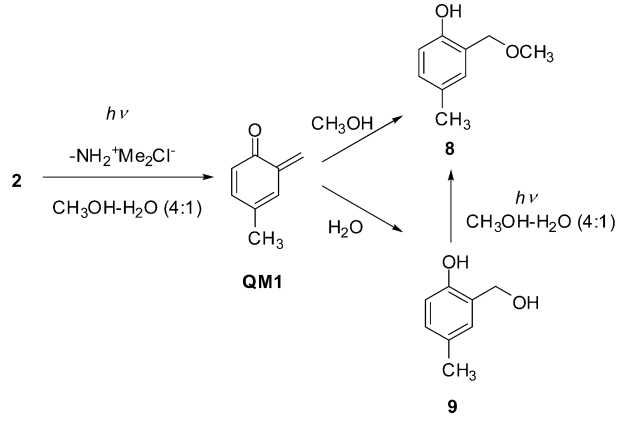

Scheme 6. Photomethanolysis of 4

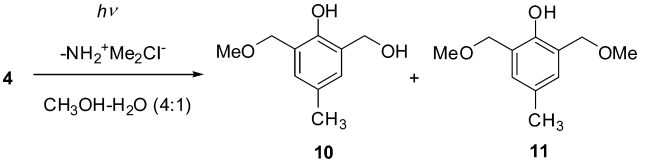

the photolysis of **1** with 85% of **8** being formed after 15 min of irradiation in the absence and presence of H_2O. In contrast, the photolysis of **2** was dependent on the water concentration where in neat CH_3OH after 15 min irradiation gave 6% of **8**, while in the presence of 10% H_2O 15% of **8** was formed. No influence of H_2O concentration on the efficiency of photomethanolysis of **1** is due to an efficient ESIPT, which is coupled with deamination and does not require a proton-accepting solvent for the reaction to occur. On the contrary, for the deamination of salt **2**, H_2O is required for the deprotonation of

DOI: 10.1021/acs.joc.5b01991
J. Org. Chem. 2015, 80, 10817–10828

phenol. It is known that phenol deprotonates faster from S_1 to H_2O clusters than to CH_3OH.[59−62]

Influence of pH on the photochemistry of **2** (Figure 3) was investigated by conducting photohydrolysis reaction at different

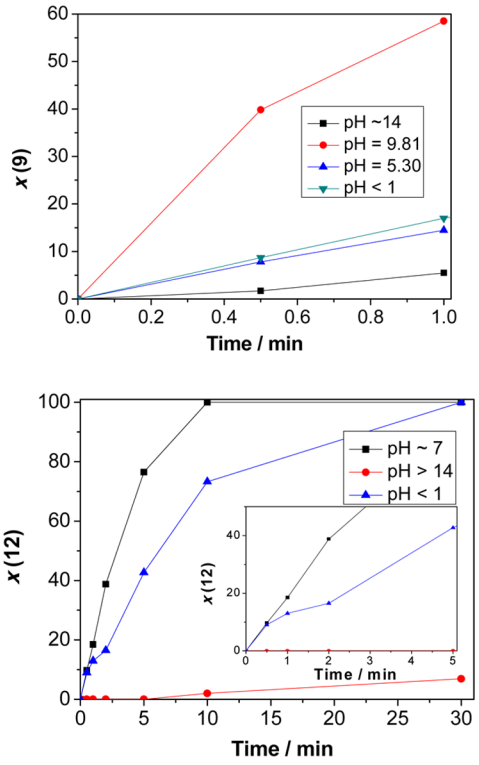

Figure 3. Dependence of the photohydrolysis efficiency on pH of **2** (top) and **5** (bottom, inset: 5 min expansion).

pH's. The pH values used were 1.0, 5.3, 9.8, and 14, corresponding to the highest concentrations of species **2**, **1zw**, and $\mathbf{1}^-$ (Scheme 3 and Figure S15, Supporting Information). The highest efficiency was observed at pH 9.8, demonstrating that the most reactive species in the photohydrolysis is the zwitterion. Photohydrolysis of salt **2** is four time less efficient then **1zw**, whereas phenolate $\mathbf{1}^-$ is the least reactive, with efficiency 10 times lower than for **1zw**. A similar photohydrolysis experiment at three pH values was conducted with **5** (Figure S21, Supporting Information). The irradiation gave compound **12**[63] that was isolated and characterized by NMR. It is interesting to note that photohydrolysis of **5** and **2** in acidic conditions wherein the amine and phenol are protonated proceeds with approximately similar efficiency. However, when phenol is in the zwitterionic form **1zw** is much more reactive than methoxy derivative **5**.

To show that **QM1** is an intermediate in the photochemistry of **2**, irradiation was performed in CH_3CN solution in the presence of ethanolamine, an ubiquitous quencher of QMs.[4,31,64−66] However, after the irradiation adduct **13** was not detected. Since ethanolamine is a base, the finding is in accord with less efficient photohydrolysis in basic conditions at pH > 12. The irradiation of **2** in neat CH_3CN was also performed in the presence of ethyl vinyl ether, which is known to react with QMs in a Diels−Alder reactions.[67] The irradiation gave chromane **14**,[68] isolated in the yield of 42%, clearly indicating the existence of **QM1** as an intermediate during the solvolysis.

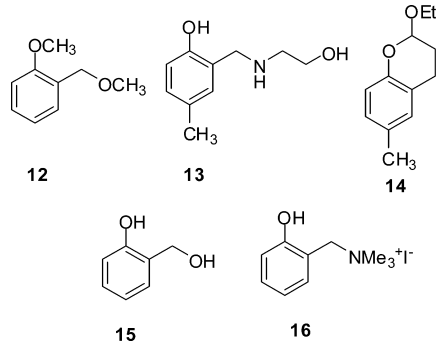

The efficiency of the photomethanolysis (Φ_R) for **1**−**4** was investigated by simultaneous use of three actinometers, ferrioxalate (Φ_{254} = 1.25),[48,69] KI/KIO_3 (Φ_{254} = 0.74),[48,70] and valerophenone (Φ_{254} = 0.65 ± 0.03).[48,71] The same method was used to determine the Φ_R for **15** and **16** (Table 3).

Table 3. Quantum Efficiency for Methanolysis (Φ_R) of 1−4, 15, and 16[a]

compd	Φ_R
1	0.11 ± 0.01
2	0.42 ± 0.03
3	0.42 ± 0.05
4	0.91 ± 0.03
15	0.20 ± 0.02[b]
16	0.40 ± 0.02[c]

[a]Measured in neutral CH_3OH-H_2O (4:1) by averaging the values obtained from using three actinometers, ferrioxalate (Φ_{254} = 1.25),[48,69] KI/KIO_3 (Φ_{254} = 0.74),[48,70] and valerophenone (Φ_{254} = 0.65 ± 0,03).[48,71] The errors correspond to the values obtained from three independent measurements, each with three actinometers. [b]Measured in neutral CH_3OH-H_2O (1:1). The literature value Φ_R = 0.23.[27] [c]Measured in neutral CH_3OH-H_2O (1:1). The literature value Φ_R = 0.98.[8] The difference is probably due to different measurement conditions.

Φ_R for **15** is within the experimental error with the reported value (Φ_R = 0.23),[27] whereas for our experimental conditions Φ_R for **16** is much lower than reported (Φ_R = 0.98).[8] It is interesting to note that methanolysis of alcohol **15** is about two times more efficient than that of amine **1**. Transformation to salts **2** and **16** increases the quantum efficiency by about four times. Bifunctional derivatives **3** and **4** undergo more efficient reactions than the corresponding **1** and **2**.

The potential thermal reactivity of **1**−**4** and **16** (10^{-3} M) in methanolysis was probed by the analysis of the CH_3OH-H_2O (1:1) solutions at different pHs (1, 7, and 14) by HPLC. The analysis revealed that **1**−**4** were stable over 15 days, whereas **16** underwent methanolysis with conversion of 23% over 15 days.

Laser Flash Photolysis. LFP measurements with excitation at 266 nm for solutions in CH_3CN and CH_3CN-H_2O (1:1) were performed for **1**−**4** to probe for the formation of QMs. In both solvents, QMs are expected to be formed, but ESPT to solvent is only possible in CH_3CN-H_2O. The transient absorption spectra of **1**−**4** in both CH_3CN and CH_3CN-H_2O (1:1) solutions are characterized by an absorption band with a maximum at ~400 nm. The transients are formed within the 10 ns laser pulse, and therefore, the kinetics for formation of the transients could not be resolved. For **1** and **2**, the spectra are shown in Figure 4 and for **4** in Figure 5 (for other spectra as well as quenching plots, see Figures S22−S40, Supporting

DOI: 10.1021/acs.joc.5b01991
J. Org. Chem. 2015, 80, 10817−10828

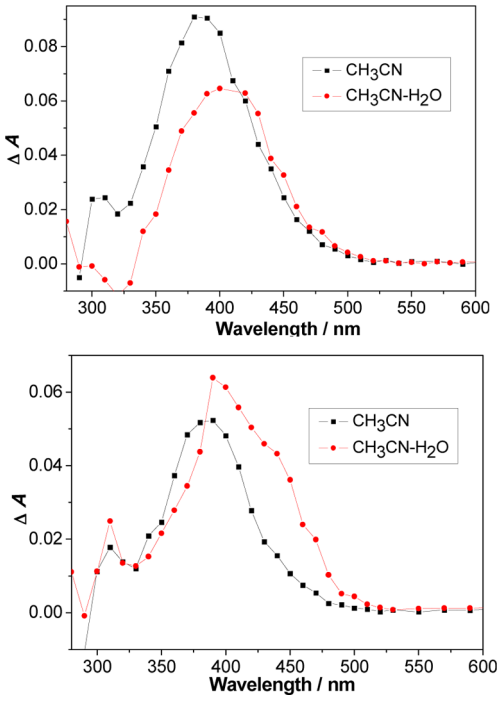

Figure 4. Transient absorption spectra in O_2 purged and optically matched ($A_{355} \approx 0.31$) solutions for **1** (top, delay = 8 μs) and **2** (bottom, delay =10 μs) in CH_3CN and in CH_3CN-H_2O. The lifetimes of the transients are compiled in Table 4.

Table 4. Lifetimes of QM1-QM4 Measured by LFP in O_2-Purged CH_3CN or CH_3CN-H_2O[a]

compd	τ (CH_3CN) (ms)	τ (CH_3CN-H_2O) (ms)
QM1	5 ± 1[b]	2.5 ± 0.2[b]
	200 ± 20[c]	105 ± 10[c]
QM3	2.0 ± 0.2	3 ± 1
QM4	0.12 ± 0.01	14 ± 2 and 135 ± 5[d]

[a]The LFP system was adapted to measure ms lifetimes.[72] [b]Measured for **1**. [c]Measured for **2**. [d]The decay kinetics were fit to sum of two exponentials.

Information). The transients decayed to the baseline with unimolecular kinetics, except for **4** in CH_3CN-H_2O where the decay was fit to a sum of two exponentials (see below). The presence of O_2 did not affect the efficiency of the formation of the transients and neither did it affect the decay rates, in agreement with the formation of transients from the singlet excited state and the formation of transients that do not react with O_2. The transients were assigned to **QM1**, **QM3**, and **QM4** based on precedent literature with respect to the position of transient absorption maximum, the decay kinetics,[8,26,27] and the lack of influence of O_2 on the decay kinetics.

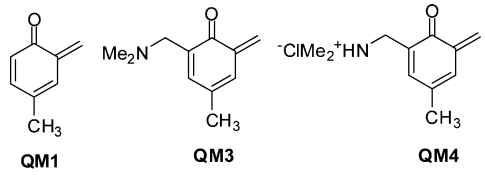

QM1 **QM3** **QM4**

The deamination of both cresols **1** and **2** gives rise to the same **QM1**. Cresol **1** bears a nucleophilic amine that is not present in salt **2**. As a consequence, **QM1** formed from **1** has a 40× shorter lifetime than from **2** due to reaction of **QM1** with

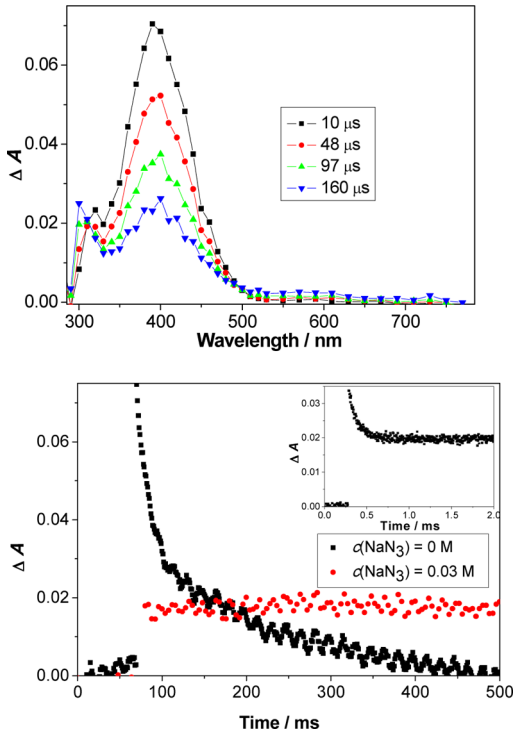

Figure 5. (Top) Transient absorption spectra of **4** in O_2-purged CH_3CN. (Bottom) Decay of the transient absorption at 420 nm in CH_3CN-H_2O (1:1) solution of **4** ($c = 6 \times 10^{-4}$ M) without quencher and in the presence of NaN_3 (0.03 M) (Inset: decay at 420 nm in the presence of 0.03 M NaN_3 at short time scale.)

dimethylamine, which quenches **QM1**. The difference in lifetimes for **QM1** corresponds to the quenching rate constant with dimethylamine of approximately 4×10^6 M^{-1} s^{-1} (assuming 10% conversion of **1** to **QM1** by laser pulse at the concentration of **1** at 5×10^{-4} M). Addition of H_2O to the CH_3CN solution changed the efficiency of the transient formation, judged from the intensity of the transient absorbance immediately after the laser pulse when solutions with the same absorbance at the excitation wavelength are compared. Thus, **QM1** is formed 1.5× more efficiently from **1** in aprotic solution, whereas for salt **2** the reaction is 1.2× more efficient in the presence of H_2O. This result is in agreement with the fluorescence measurements and influence of H_2O on the methanolysis efficiency (see above). All these results clearly indicate that protic solvent increases the rate of deamination of the salts, whereas it decreases the rate for the amines. The decay kinetics of **QM1**−**QM3** are slower in CH_3CN than in the presence of H_2O, which is in agreement with the reaction of QMs with H_2O.[4,26−28,31,64−66,73−75]

Contrary to **QM1** and **QM3**, **QM4** exhibits about 100× shorter lifetime in CH_3CN than in aqueous solution (Figure 5). This shorter lifetime of **QM4** in CH_3CN is probably due to intramolecular protonation of the carbonyl oxygen by the ammonium salt along the intramolecular H bond, rendering **QM4** (or the resulting **cat**$^+$, Scheme 7) more reactive with nucleophiles. Acid catalysis in the hydration reactions of QMs has been demonstrated.[26,73−77] Addition of H_2O to the CH_3CN solution probably disrupts the intramolecular H bond in **QM4**, leading to the less efficient protonation of the QM carbonyl and longer lifetime. Interestingly, the decay of **QM4** in aqueous solution was fit to the sum of two exponentials (Figure 5, bottom). This finding was explained

DOI: 10.1021/acs.joc.5b01991
J. Org. Chem. 2015, 80, 10817−10828

Scheme 7. Reactions of QM4

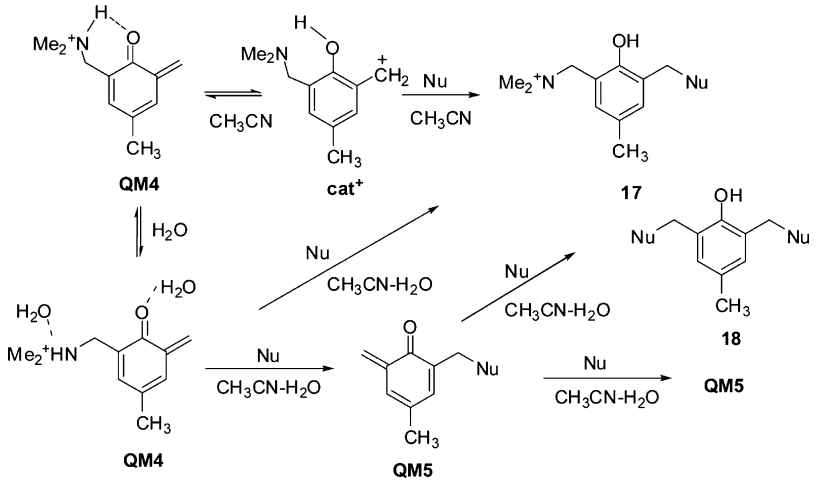

Table 5. Quenching Rate Constants (k_q (M^{-1} s^{-1})) Obtained by LFP

quencher	QM1	QM3	QM4
CH_3OH[c]	430 ± 40[a]		
	d		
ethanolamine[e]	(9.7 ± 0.2) × 10^4[a]	(6.8 ± 0.4) × 10^4	(5.5 ± 0.2) × 10^4[f]
	(1.0 ± 0.2) × 10^5[b]		
NaN_3[e]	(5.0 ± 0.1) × 10^6[a]	(3.6 ± 0.1) × 10^6	(1−10) × 10^6[g]
	(4.9 ± 0.3) × 10^6[b]		
EVE[e]	600−800[a]	700−1300	
	d		

[a]The transient formed from **1**. [b]The transient formed from **2**. [c]Measured in CH_3CN. [d]The transient was too long-lived for the accurate measurement of the quenching rate constant. [e]Measured in CH_3CN−H_2O (1:1). [f]Measured in CH_3CN−H_2O (1:1). The decay becomes single exponential in the presence of a base. [g]The short decay component is quenched (only order of magnitude estimate was possible because of poor quality of quenching plot, Figure S39 in the Supporting Information), whereas the slow-decaying transient becomes long-lived with a lifetime >10 s.

by two reactions of **QM4**, one leading to new **QM5**, and the other to adduct **17** (Scheme 7). Since the spectra of **QM4** and **QM5** overlap, biexponential decay of the transient absorption was observed. The short decay time probably corresponds to **QM4** and the long one to **QM5**. Such a biexponential decay was not observed for **QM3** since the amine is a worse leaving group compared to the ammonium salt. That is, upon attack of nucleophile to **QM3**, only adducts can be formed and not a QM as shown in Scheme 7 for the protonated derivative **QM4**.

Additional evidence for the assignment of the observed transients to QMs was obtained through quenching studies. The quenching was conducted with nucleophiles CH_3OH, ethanolamine, NaN_3, and ethyl vinyl ether (EVE) that reacts with QMs in a Diels−Alder reaction (Figures S22−S40, Supporting Information). Some of the quenching rate constants are only approximate values due to imprecise kinetic measurements at long time scales (Table 5). All values are in agreement with the precedent in the literature.[4,8,76,77] In the quenching experiment of **QM4** it is interesting that addition of NaN_3 quenches only the short decay for which only an estimate could be provided of (1−10) × 10^6 M^{-1} s^{-1} due to poor quality of the quenching plot, whereas the long decay component (τ = 135 ± 5 ms) became longer lived (τ > 10 s). This finding was explained by reaction of **QM5** with N_3^- in which N_3^- is also the leaving group (Scheme 7). The reaction does not give rise to a new product since **QM5** is regenerated, which leads to the observed long-lived transient absorption. However, formation of **18** is eventually expected leading to the decay of this transient.

DISCUSSION

The results show unequivocally that the mechanism for the photodeamination of amines **1** and **3** can be different from the photodeamination of salts **2** and **4** depending on the solvent system, showing that the presence of a basic site in **1** and **3** leads to efficient ESIPT while for the salts that do not have this basic site the proton transfer has to occur with the solvent. Such a difference has a direct impact on the photodeamination reactivity in hydrophobic sites of biological systems where the availability of water may be limited.

The different reactivities will be illustrated for amine **1** and the corresponding salt **2**. On excitation of **1** in aprotic solvent (CH_3CN), adiabatic ESIPT takes place along the intramolecular H bond and gives zwitterion **1zw**, which was detected by fluorescence spectroscopy as a species that emits at a longer wavelength. Due to efficient ESIPT, the singlet excited state lifetime of **1** is expected to be short and the fluorescence quantum yield is low. Formation of **1zw** in S_1 is followed by deamination, also occurring from S_1. Namely, **1zw** is antiaromatic in S_1,[78,79] leading to the formation of the more stable **QM1** (Scheme 8). In aqueous solution at pH 7, the amine is protonated (Table 2) and the dominant species is cation **2**. Therefore, ESIPT cannot take place. Instead, ESPT to proton-accepting solvent upon excitation gives **1zw**, which is the reactive species in the photodeamination. The quantum

DOI: 10.1021/acs.joc.5b01991
J. Org. Chem. 2015, 80, 10817−10828

Scheme 8. Mechanism of QM1 Formation from 1

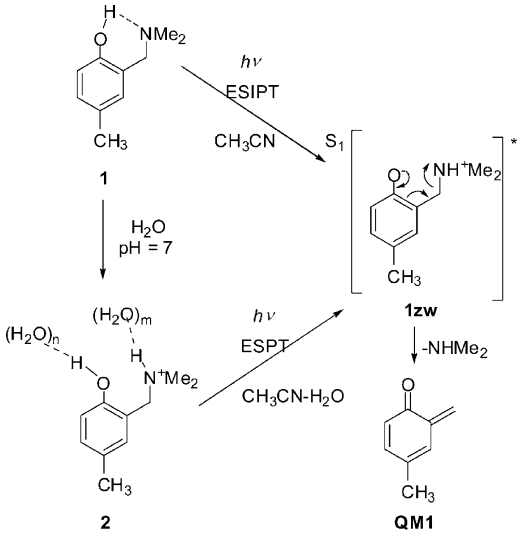

yield for the formation of **QM1** in a protic solvent is 1.5× lower than in neat CH_3CN, as demonstrated by LFP, suggesting that ESIPT is more efficient than ESPT to solvent, both of which are coupled with deamination. **QM1** ultimately gives adducts with nucleophiles or undergoes Diels–Alder reaction with dienophiles.

ESPT to CH_3CN cannot take place due to its weak proton-accepting properties.[42,43,49,50,59−62] Moreover, ESIPT is not possible in salt **2**, which does not contain a basic site. Since photosolvolysis of ether **5** takes place, but cannot involve formation of QMs, it is highly conceivable that photosolvolysis of **5** and deamination of **2** in aprotic solvent proceed via a similar mechanism. Most probably, excitation of **2** to S_1 in aprotic solvent leads first to the cleavage of the ammonium giving cation **18** (Scheme 9), followed by the deprotonation in the attack of dimethylamine to give **QM1**. We have no spectral evidence for the formation of cation **18**, and at this point it remains undetected.

Scheme 9. Mechanism of QM1 Formation from 2

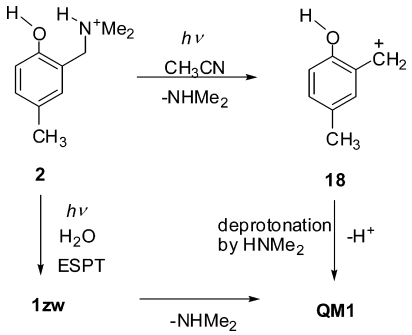

The efficiency of the reaction is related to the prototropic form of the reactant molecule. When **2** is dissolved in aqueous solvent at pH 7, the photodeamination takes place more efficiently due to proton transfer to the solvent and follows the same mechanism as discussed for **1**. Increase of the pH leads to the formation of **1zw**, which further increases the efficiency of photodeamination (Scheme 9). However, above pH 11, the photodeamination is the least efficient. At such a high pH, anion $\mathbf{1}^-$ is the dominant species and is not very reactive since dimethylamine is a poor leaving group.

The mechanism of QM formation from bifunctional derivatives **3** and **4** follows the same mechanism in aprotic solvent, as discussed for **1** and **2**. However, in aqueous solution one more acid–base equilibrium exists. Thus, in aqueous solution at pH 7, the diamine is present in its monocationic form $\mathbf{3}^+$, which is the most reactive form in the deamination reaction. Therefore, the deamination takes place very efficiently, as judged from the methanolysis quantum yield for **4** (Φ_R = 0.91). Moreover, an additional electron-donor group in **QM3** and electron-acceptor in **QM4** change the reactivity of **QM4** compared to **QM1**, as demonstrated in the reaction with azide, and in line with precedent in the literature.[56] Particularly interesting is the reactivity of **QM4** which bears a very good leaving group. Thus, attack of nucleophiles gives rise to the new **QM5** or to adducts **17**. This finding is particularly important for the application of **QM4** in biological systems for the formation of thermodynamically most stable DNA cross-links. Reversible alkylation of DNA by QMs and "immortalization of QM" by DNA as a nucleophile has been postulated,[16,80−82] wherein initial formation of DNA alkylation products formed under kinetic control follows repeated capture and release of the QM until the thermodynamically most stable products are formed. However, to the best of our knowledge, a spectral evidence for the competing reactions of bifunctional QMs has not yet been provided. Our results cannot completely rule out other mechanistic scenarios that lead to solvolysis products and do not involve QMs. However, if they take place they should be very inefficient.

■ CONCLUSION

Cresol derivatives **1**–**4** were synthesized and their acid–base properties, photophysics, and photochemical reactivity in photodeamination reactions investigated. On excitation to S_1 the cresols become more acidic. Therefore, amine derivatives **1** and **3** in aprotic solvent in S_1 undergo ESIPT giving zwitterions **1zw** and **3zw**, which subsequently in the photodeamination reaction give **QM1** and **QM3**, respectively. Salts **2** and **4** cannot deactivate by ESIPT. However, photodeamination from these salts takes place wherein the ammonium group is presumably cleaved first to give undetected benzyl cation, and subsequently, deprotonation gives **QM1** and **QM4**. Although **1** and **2** give the same **QM1**, the lifetime of the transient is different as well as the overall efficiency in the photosolvolysis. **QM1** exhibits shorter lifetime when formed from **1** (τ in CH_3CN = 5 ms) then from **2** (τ in CH_3CN = 200 ms) due to the reaction with eliminated dimethylamine. In aqueous solvent, deamination depends largely on the prototropic form of the molecule. The most efficient deamination takes place when the amine is in the zwitterionic form (pH 9–11) and the diamine is in the monocationic form (pH 7–9). **QM1**, **QM3**, and **QM4** were detected by LFP (λ_{max} = 400 nm, τ = 0.1–200 ms), and the rate constants of their reactions with nucleophiles were measured. Bifunctional **QM4** with a good leaving group undergoes two types of reactions with nucleophiles, giving adducts or new QMs. The result is of significant importance for biological systems where bifunctional QMs are used in the DNA cross-linking. Revealing differences in reactivity of salts and amines studied in this work is important in the use of QMs for alkylation of proteins wherein a hydrophobic microenvironment or proximity of acidic or basic amino acid residues can significantly alter kinetics of their formation and decay.

DOI: 10.1021/acs.joc.5b01991
J. Org. Chem. 2015, 80, 10817–10828

Moreover, we have shown herein that deamination in aqueous solution can be controlled by pH, which could have some implications in biology, for example, in controlled drug delivery. In principle, instead of methyl groups on the amine, salt **2** can be substituted with a drug, such as amantadine or memantine, that would efficiently undergo photodeamination and drug release only in the pH region 8.5−10.5.

EXPERIMENTAL SECTION

General Methods. ^{1}H and ^{13}C NMR spectra were recorded at 300 or 600 MHz at rt using TMS as a reference, and chemical shifts were reported in ppm. Melting points were determined using a Mikroheiztisch apparatus and were not corrected. IR spectra were recorded on a spectrophotometer in KBr, and the characteristic peak values are given in cm^{-1}. HRMS were obtained on a MALDI TOF/TOF instrument. Irradiation experiments were performed in a reactor equipped with 11 lamps with output at 300 nm or a reactor equipped with 8 lamps. During the irradiations, the irradiated solutions were continuously purged with Ar and cooled by a tap water finger-condenser. Solvents for irradiations were of HPLC purity. Chemicals were purchased from the usual commercial sources and were used as received. Solvents for chromatographic separations were used as delivered from the supplier (p.a. or HPLC grade) or purified by distillation (CH_2Cl_2).

*2-[(N,N-Dimethylamino)methyl]-4-methylphenol (**1**).* In a round-bottom flask (50 mL), *p*-cresol (163 mg, 1.51 mmol) and anhydrous K_2CO_3 (313 mg, 2.26 mmol) were suspended in CH_2Cl_2 (10 mL). *N*,*N*-Dimethylmethyleneiminium chloride (142 mg, 1.52 mmol) was added, and the reaction mixture was stirred at rt for 16 h. The next day, the reaction mixture was filtered and the solid was washed with ethyl acetate. The solvent was removed on a rotary evaporator to furnish a crude oily product, which was purified on a column of alumina (act. IV) using CH_2Cl_2 as eluent to afford 222 mg (93%) of pure **1** as a colorless viscous oil. Characterization of **1** is in accord with the precedent literature:[83] ^{1}H NMR ($CDCl_3$, 300 MHz) δ 6.96 (dd, 1H, J = 8.1, 1.2 Hz), 6.76 (d, 1H, J = 1.2 Hz), 6.72 (d, 1H, J = 8.1 Hz), 3.59 (s, 2H), 2.31 (s, 6H), 2,23 (s, 3H); ^{13}C NMR ($CDCl_3$, 75 MHz) δ 155.5, 128.9, 128.7, 127.8, 121.5, 115.6, 62.8, 44.4, 20.3.

*2-[(N,N-Dimethylamino)methyl]-4-methylphenol Hydrochloride (**2**).* To the solution of amine **1** (200 mg) in CH_2Cl_2−Et_2O (1:1, 5 mL) was added a saturated solution of HCl in Et_2O, whereupon white precipitate was formed. The precipitate was filtered and washed with Et_2O (3 × 10 mL). Drying in a desiccator over KOH afforded 222 mg (93%) of **2** in the form of colorless crystals: ^{1}H NMR (DMSO-d_6, 300 MHz) δ 10.1 (s, 1H), 10.0 (br s, 1H), 7.23 (d, 1H, J = 1.8 Hz), 7.07 (dd, 1H, J = 8.2, 1.8 Hz), 6.90 (d, 1H, J = 8.2 Hz), 4.15 (d, 2H, J = 4.9 Hz), 2.69 (d, 6H, J = 4.6 Hz), 2.22 (s, 3H); ^{13}C NMR (DMSO-d_6, 150 MHz) δ 154.2, 132.9, 131.4, 127.6, 116.1, 115.5, 54.6, 41.7, 19.9.

*2,6-Bis[(N,N-dimethylamino)methyl]-4-methylphenol (**3**).* In a round-bottom flask (50 mL) equipped with a condensor, *p*-cresol (2.34 g, 21.6 mmol), dimethylamine (40% aq, 8.2 mL, 64.8 mmol), and formalin (37% aq, 4.2 mL, 56 mmol) were mixed and heated at reflux over 2 h. After the mixture was cooled to rt, solid NaCl was added, whereupon the layers were separated. The upper organic layer was dried with anhydrous Na_2SO_4, and the solid was filtered off. The crude product was purified on a column of alumina (act. IV/V) using CH_2Cl_2 as eluent to afford 4.19 g (87%, lit.[84] 39%) of colorless oil. Characterization of **3** is in accord with the precedent literature:[84] ^{1}H NMR ($CDCl_3$, 300 MHz) δ 6.83 (s, 2H), 3.50 (s, 4H), 2.29 (s, 12H), 2.23 (s, 3H); ^{13}C NMR ($CDCl_3$, 300 MHz) δ 154.1 (s), 129.1 (d), 127.1 (s), 122.9 (s), 60.3 (t), 44.7 (q), 20.3 (q).

*2,6-Bis[(N,N-dimethylamino)methyl]-4-methylphenol Hydrochloride (**4**).* To a solution of amine **3** (50 mg) in CH_2Cl_2−Et_2O (1:1, 5 mL) was added a saturated solution of HCl in Et_2O, whereupon a white precipitate was formed. The precipitate was filtered through a sinter and washed with Et_2O (3 × 10 mL). The crude product was purified by crystallization from CH_3OH−Et_2O at 4 °C. Pure product **4** (55 mg, 82%) was obtained in the form of colorless crystals: ^{1}H NMR (DMSO-d_6, 600 MHz) δ 7.41 (s, 2H), 4.34 (s, 4H), 2.72 (s, 12H), 2.25 (s, 3H); ^{13}CNMR (DMSO-d_6, 150 MHz) δ 153.3, 135.1, 129.1, 119.5, 54.5, 41.6, 19.9.

*2-Methoxybenzaldehyde (**6**).* Salicylaldehyde (1.2 g, 10 mmol), Na_2CO_3 (1.3 g, 12 mmol), THF (60 mL), and MeOH (15 mL) were mixed in a two-necked round flask (100 mL) equipped with a reflux condenser. MeI (1.9 mL, 30 mmol) was added dropwise, and the resulting suspension was refluxed overnight. The reaction mixture was poured on water (200 mL) and extracted with CH_2Cl_2 (3 × 30 mL). Combined organic extracts were dried on $MgSO_4$ and filtered, and the solvent was removed on a rotary evaporator to obtain 1.29 g (95%) of product in the form of yellowish oil. The product was used in the next step without further purification. NMR spectra of **6** are in accord with the known spectra:[40] ^{1}H NMR ($CDCl_3$, 600 MHz) δ 10.5 (s, 1H), 7.83 (dd, 1H, J = 7.5 and 1.7 Hz), 7.57−7.53 (m, 1H), 7.03 (t, 1H, J = 7.5 Hz), 6.99 (d, 1H, J = 8.4 Hz), 3.93 (s, 3H); ^{13}C NMR ($CDCl_3$, 75 MHz) δ 189.7 (d), 161.7 (s), 135.8 (d), 128.5 (d), 124.8 (s), 120.6 (d), 111.5 (d), 55.5 (q).

*2-(N,N-Dimethylamino)methyl-1-methoxybenzene Hydrochloride (**5**).* Compound **6** (272 mg, 2 mmol) and 40% aqueous dimethylamine (1 mL, 7.9 mmol) were dissolved in absolute methanol (20 mL) in a round-bottomed flask and stirred vigorously overnight. The in situ formed Schiff base underwent reductive amination under a hydrogen atmosphere (balloon, 1 atm) and PtO_2 catalyst (20 mg, 0.09 mmol). The mixture was then filtered and the solvent removed on a rotary evaporator to afford a brown oil. The product was purified on a short column of silica gel using hexane/ethyl acetate (9:1) as eluent to afford 39 mg (55%) of yellow oil (7), which was immediately converted to the corresponding hydrochloride salt **5** by adding a saturated solution of HCl in MeOH. The salt was recrystallized three times from acetonitrile/ether (7:3) to obtain 250 mg (62%) of the pure product in the form of a white solid: mp 147−148 °C (lit.[39] mp 149 °C); ^{1}H NMR (D_2O, 300 MHz) δ 7.60−7.52 (m, 1H), 7.41 (dd, 1H, J = 7.5, 1.6 Hz), 7.16 (d, 1H, J = 8.3 Hz), 7.10 (t, 1H, J = 7.5 Hz), 4.33 (s, 2H), 3.93 (s, 3H), 2.86 (s, 6H); ^{13}C NMR (D_2O, 75 MHz) δ 158.6 (s), 133.0 (d), 132.8 (d), 121.6 (d), 118.3 (s), 112.0 (d), 58.0 (t), 56.1 (q), 43.1 (q).

Irradiation Experiments. *4-Methyl-2-methoxymethylphenol (**8**).* A quartz vessel was filled with a solution of **2** (17 mg, 0.084 mmol) in CH_3OH−H_2O (4:1, 50 mL), and the solution was purged with N_2 (20 min), sealed, and irradiated in a reactor at 300 nm with eight lamps over 30 min. After the irradiation, the solvent was removed on a rotary evaporator, and the residue purified on a column of silica using CH_2Cl_2 as eluent to afford 10 mg (77%) of **8** in the form of colorless oil. Characterization of product **8** is in accord with the precedent literature:[57] ^{1}H NMR ($CDCl_3$, 600 MHz) δ 7.21 (s, 1H), 7.00 (d, 1H, J = 8.1 Hz), 6.81 (br s, 1H), 6.78 (d, 1H, J = 8.1 Hz), 4.62 (s, 2H), 3.42 (s, 3H), 2.25 (s, 3H); ^{13}C NMR ($CDCl_3$, 150 MHz) δ 153.8 (s), 129.8 (d), 128.9 (s), 128.6 (d), 121.6 (s), 116.2 (d), 74.1 (t), 58.0 (q), 20.6 (q).

*Preparative Irradiation of 2,6-Bis[(N,N-dimethylamino)methyl]-4-methylphenol Hydrochloride (**4**).* A quartz vessel was filled with a solution of **4** (100 mg, 0.34 mmol) in CH_3OH−H_2O (4:1, 100 mL), and the solution was purged with Ar (20 min) and irradiated in a reactor at 300 nm with 11 lamps over 20 min. During the irradiation, the solution was continuously purged with Ar and cooled with a finger condenser. After the irradiation, the solvent was removed on a rotary evaporator and the residue purified by a preparative HPLC on a C18 column (250 × 5 mm, 5 μm) and MeOH−H_2O (6:4 + 0.5% HOAc) eluent to afford pure products **10** and **11** (both as thick colorless oils).

*6-Hydroxymethyl-4-methyl-2-methoxymethylphenol (**10**):* 4 mg (7%); ^{1}H NMR ($CDCl_3$, 300 MHz) δ 6.95 (s, 1H), 6.83 (s, 1H), 4.71 (s, 2H), 4.62 (s, 2H), 3.44 (s, 3H), 2.25 (s, 3H); ^{13}C NMR ($CDCl_3$, 150 MHz) δ 152.0 (2C, s, d), 128.9 (d), 128.8 (s), 128.1 (d), 127.0 (s), 122.6 (s), 71.7 (t), 62.6 (t), 58.2 (q), 20.3 (q); IR (KBr, cm^{-1}): 3400 (vs), 2921 (s), 2868 (m), 2825 (w), 1719 (w), 1650 (w), 1617 (s), 1484 (vs), 1382 (s), 1228 (s), 1159 (m), 1090 (s), 1032 (w), 867 (m); HRMS (MALDI-TOF) m/z [M − H]$^+$ calcd for ($C_{10}H_{14}O_3$) 181.0870, found 181.0867.

*4-Methyl-2,6-bis(methoxymethyl)phenol (**11**):* 20 mg (30%);[58] ^{1}H NMR ($CDCl_3$, 600 MHz) δ 7.55 (br.s, 1H), 6.92 (s, 2H), 4.56 (s, 4H),

DOI: 10.1021/acs.joc.5b01991
J. Org. Chem. 2015, 80, 10817−10828

3.43 (s, 6H), 2.25 (s, 3H); ^{13}C NMR ($CDCl_3$, 150 MHz) δ 151.8 (s), 128.9 (d), 128.6 (s), 123.2 (s), 71.8 (q), 58.1 (q).

*1-Methoxy-2-methoxymethylbenzene (**12**).* A quartz vessel was filled with a solution of **7** (20 mg, 0.1 mmol) in CH_3OH–H_2O (4:1, 35 mL), and the solution was purged with N_2 (20 min), sealed, and irradiated in a reactor at 300 nm with eight lamps over 60 min. After the irradiation, the solvent was removed on a rotary evaporator and the residue purified on a column of silica using CH_2Cl_2 as eluent to afford 11 mg (59%) of **12** in the form of a colorless oil. Characterization of product **12** is in accord with the precedent literature:[63] ^{1}H NMR ($CDCl_3$, 300 MHz) δ 7.34 (d, 1H, J = 7.4 Hz), 7.30–7.22 (m, 1H), 6.95 (t, 1H, J = 7.4 Hz), 6.87 (d, 1H, J = 8.1 Hz), 4.50 (s, 2H), 3.83 (s, 3H), 3.42 (s, 3H); ^{13}C NMR ($CDCl_3$, 150 MHz) δ 157.1 (s), 129.0 (d), 128.6 (d), 126.4 (s), 120.3 (d), 110.1 (d), 69.4 (t), 58.2 (q), 55.3 (q).

*2-Ethoxy-6-methylchromane (**14**).* A quartz vessel was filled with a solution of **2** (20 mg, 0.1 mmol) in CH_3CN (20 mL). The solution was purged with Ar (20 min), and ethyl vinyl ether (5 mL, 20.9 mmol) was added. The solution was irradiated in a reactor at 300 nm with 11 lamps over 30 min. During the irradiation, the solution was continuously purged with Ar and cooled with a finger condenser. After the irradiation, the solvent was removed on a rotary evaporator and the residue purified on a column of silica gel using CH_2Cl_2 as eluent to afford pure product **14** (8 mg, 42%) in the form of colorless oil. Characterization of **14** is in accord with the precedent literature:[68] ^{1}H NMR ($CDCl_3$, 600 MHz) δ 6.90 (d, 1H, J = 8.1 Hz), 6.86 (s, 1H), 6.72 (d, 1H, J = 8.1 Hz), 5.22 (t, 1H, J = 2.9 Hz), 3.90–3.84 (m, 1H), 3.66–3.60 (m, 1H), 2.97–2.90 (m, 1H), 2.62–2.56 (m, 1H), 2.25 (s, 3H), 2.04–1.99 (m, 1H), 1.96–1.90 (m, 1H), 1.18 (t, 3H, J = 7.1 Hz); ^{13}C NMR ($CDCl_3$, 150 MHz) δ 149.9 (s), 129.6 (s), 129.5 (d), 127.7 (d), 122.2 (s), 116.5 (d), 96.8 (d), 63.4 (t), 26.6 (t), 20.4 (t), 20.3 (q), 15.0 (q).

Measurements of Photomethanolysis Quantum Yields. The quantum yield of the photomethanolysis reaction was determined by use of three actinometers during the same experiment: ferrioxalate (Φ_{254} = 1.25),[48,69] KI/KIO_3 (Φ_{254} = 0.74),[48,70] and valerophenone (Φ_{254} = 0.65 ± 0.03).[48,71] The measurement of irradiance was described in detail in our previous work,[85] and the same procedures were employed in this work. The solutions of compounds **1**–**4** in CH_3OH–H_2O (4:1) and **15** and **16** in CH_3OH–H_2O (1:1) were prepared, and their concentrations were adjusted to have absorbances of 0.4–0.8 at 254 nm. The solutions were purged with a stream of N_2 (20 min each) and then sealed with a cap. Solution of compounds and actinometers were irradiated in quartz cuvettes (each have same geometry) at the same time with one lamp (254 nm). Similar values of irradiance were obtained for all three actinometers. For compounds **1**–**4**, **15**, and **16**, consumption of reactant was measured (HPLC), and this value was used for calculating quantum yields. Measurements were done three times in three independent experiments, and the mean value is reported.

Steady-State and Time-Resolved Fluorescence Measurements. Steady-state measurements were performed on two different fluorimeters. The samples were dissolved in CH_3CN or CH_3CN–H_2O (1:1), and the concentrations were adjusted to absorbances of less than 0.1 at excitation wavelengths of 260, 270, or 280 nm. Solutions were purged with nitrogen for 30 min prior to analysis. Measurements were performed at 20 °C. Fluorescence quantum yields were determined by comparison of the integral of the emission bands with the one of anisole in cyclohexane (Φ_f = 0.29).[48] Typically, three absorption traces were recorded (and averaged), and three fluorescence emission traces were collected by exciting the sample at three different wavelengths. Three quantum yields were calculated (eq S1, Supporting Information), and the mean value was reported.

Fluorescence decays, collected over 1023 time channels, were obtained on a single photon counter using a light-emitting diode for excitation at 260 nm. The instrument response functions, using LUDOX as the scatterer, were recorded at the same wavelengths as the excitation wavelength and had a half width of ~0.2 ns. Emission decays for samples in CH_3CN solution were recorded at 310 nm for **1** and **2** and at 320 nm for **3** and **4**. The counts in the peak channel were 2 × 10^2 for **1** and **3** and 5 × 10^2 for **2** and **4** because the fluorescence intensity was low and further accumulation of data was not possible. The time increment per channel was 0.020 ns. Obtained histograms were fit as sums of exponentials using global Gaussian-weighted nonlinear least-squares fitting based on Marquardt–Levenberg minimization implemented in the Fast software package from the instrument. The fitting parameters (decay times and pre-exponential factors) were determined by minimizing the reduced χ^2, and graphical methods were used to judge the quality of the fit that included plots of the weighted residuals vs channel number.

Alternatively, a single-photon-counting setup was used that consisted of 267 nm pulsed light emitting diode with a repetition rate of 10 MHz. The instrument response function of this setup was 250 ps. The time traces (4096 channels) were analyzed by software from the instrument (for more details, see the Supporting Information).

Determination of pK_a and pK_a * for 2 and 4. *UV–vis Titration.* A solution of compound **2** (c = 2.72 × 10^{-4} M) or **4** (c = 2.66 × 10^{-4} M) was prepared in H_2O (120 mL). That solution was titrated with a diluted solution of NaOH until pH 13 was reached. The measurements were performed at 25 °C. The resulting UV–vis spectra were processed by multivariate nonlinear regression analysis using the SPECFIT program. In the analysis, a surface was fit that is defined by all UV–vis spectra from 225 to 350 nm at different pH values.

Fluorescence Titration. The titration was performed by mixing a buffer solution ($HClO_4$, citrate, and phosphate) in a concentration range of 10–100 mM to the same volume of CH_3CN (pH from 1.0 to 9.2). The concentrations of **2** and **4** were 6.0 × 10^{-4} and 7.0 × 10^{-4} M, respectively. In order to get the best spectra, the excitations were performed near the isosbestic point (290 nm for **2** and 295 nm for **4**; the bandwidth of the excitation and emission monochromators were set to 2 nm), so that absorbance in the S_0 was pH independent. The baseline corrected peak maxima found were plotted against the pH value to estimate the pK* values.

Laser Flash Photolysis. All LFP studies were performed on a system previously described[86] using as an excitation source a pulsed Nd:YAG laser at 266 nm (<20 mJ per pulse), with a pulse width of 10 ns. Static cells (7 mm × 7 mm) were used, and the solutions were purged with nitrogen or oxygen for 20 min prior to performing the measurements. Absorbances at 266 nm were ~0.3–0.5. For the collection of decays at long time scales, a modification of the setup was used wherein the probing light beam from the Xe lamp was not pulsed, as previously described.[72]

■ ASSOCIATED CONTENT

Supporting Information

The Supporting Information is available free of charge on the ACS Publications website at DOI: 10.1021/acs.joc.5b01991.

UV–vis and fluorescence spectra of **1**–**4**, pH titration data for **2** and **4**, selected experimental procedures and results, LFP data, and ^{1}H and ^{13}C NMR spectra (PDF)

■ AUTHOR INFORMATION

Corresponding Author

*E-mail address: nbasaric@irb.hr.

Notes

The authors declare no competing financial interest.

■ ACKNOWLEDGMENTS

These materials are based on work financed by the Croatian Foundation for Science (HRZZ, IP-2014-09-6312), the Natural Sciences and Engineering Research Council (NSERC) for CB (RGPIN-121389-2012), the University of Victoria (UVIC), and EPA-Austria. N.B. and Đ.Š. thank Dr. K. Mlinarić-Majerski for the useful discussions. N.B. thanks UVIC for support and Professor P. Wan for support and useful discussions.

DOI: 10.1021/acs.joc.5b01991
J. Org. Chem. 2015, 80, 10817–10828

REFERENCES

(1) Rokita, S. E., Ed. *Quinone Methides*; Wiley: Hoboken, 2009.
(2) Freccero, M. *Mini-Rev. Org. Chem.* **2004**, *1*, 403−415.
(3) Wang, P.; Song, Y.; Zhang, L.; He, H.; Zhou, X. *Curr. Med. Chem.* **2005**, *12*, 2893−2913.
(4) Basarić, N.; Mlinarić-Majerski, K.; Kralj, M. *Curr. Org. Chem.* **2014**, *18*, 3−18.
(5) Percivalle, C.; Doria, F.; Freccero, M. *Curr. Org. Chem.* **2014**, *18*, 19−43.
(6) Wang, H. *Curr. Org. Chem.* **2014**, *18*, 44−60.
(7) McCracken, P. G.; Bolton, J. L.; Thatcher, G. R. J. *J. Org. Chem.* **1997**, *62*, 1820−1825.
(8) Modica, E.; Zanaletti, R.; Freccero, M.; Mella, M. *J. Org. Chem.* **2001**, *66*, 41−52.
(9) Arumugam, S.; Guo, J.; Mbua, N. E.; Friscourt, F.; Lin, N.; Nekongo, E.; Boons, G.-J.; Popik, V. V. *Chem. Sci.* **2014**, *5*, 1591−1598.
(10) Rokita, S. E.; Yang, J.; Pande, P.; Greenberg, W. A. *J. Org. Chem.* **1997**, *62*, 3010−3012.
(11) Veldhuyzen, W. F.; Shallop, A. J.; Jones, R. A.; Rokita, S. E. *J. Am. Chem. Soc.* **2001**, *123*, 11126−11132.
(12) Weinert, E. E.; Frankenfield, K. N.; Rokita, S. E. *Chem. Res. Toxicol.* **2005**, *18*, 1364−1370.
(13) Chatterjee, M.; Rokita, S. E. *J. Am. Chem. Soc.* **1994**, *116*, 1690−1697.
(14) Zeng, Q.; Rokita, S. E. *J. Org. Chem.* **1996**, *61*, 9080−9081.
(15) Pande, P.; Shearer, J.; Yang, J.; Greenberg, W. A.; Rokita, S. E. *J. Am. Chem. Soc.* **1999**, *121*, 6773−6779.
(16) Veldhuyzen, W. F.; Pande, P.; Rokita, S. E. *J. Am. Chem. Soc.* **2003**, *125*, 14005−14013.
(17) Li, V. S.; Kohn, H. *J. Am. Chem. Soc.* **1991**, *113*, 275−283.
(18) Han, I.; Russell, D. J.; Kohn, H. *J. Org. Chem.* **1992**, *57*, 1799−1807.
(19) Tomasz, M.; Das, A.; Tang, K. S.; Ford, M. G. J.; Minnock, A.; Musser, S. M.; Waring, M. J. *J. Am. Chem. Soc.* **1998**, *120*, 11581−11593.
(20) Kralj, M.; Uzelac, L.; Wang, Y.-H.; Wan, P.; Tireli, M.; Mlinarić-Majerski, K.; Piantanida, I.; Basarić, N. *Photochem. Photobiol. Sci.* **2015**, *14*, 1082−1092.
(21) Bolon, D. A. *J. Org. Chem.* **1970**, *35*, 3666−3670.
(22) Qiao, G. G.-H.; Lenghaus, K.; Solomon, D. H.; Reisinger, A.; Bytheway, I.; Wentrup, C. *J. Org. Chem.* **1998**, *63*, 9806−9811.
(23) Dorrestijn, E.; Kranenburg, M.; Ciriano, M. V.; Mulder, P. *J. Org. Chem.* **1999**, *64*, 3012−3018.
(24) Yato, M.; Ohwada, T.; Shudo, K. *J. Am. Chem. Soc.* **1990**, *112*, 5341−5342.
(25) Seiler, P.; Wirz, J. *Tetrahedron Lett.* **1971**, *12*, 1683−1686.
(26) Chiang, Y.; Kresge, A. J.; Zhu, Y. *J. Am. Chem. Soc.* **2002**, *124*, 6349−6356.
(27) Diao, L.; Yang, C.; Wan, P. *J. Am. Chem. Soc.* **1995**, *117*, 5369−5370.
(28) Arumugam, S.; Popik, V. V. *J. Am. Chem. Soc.* **2009**, *131*, 11892−11899.
(29) Lukeman, M.; Wan, P. *J. Am. Chem. Soc.* **2002**, *124*, 9458−9464.
(30) Basarić, N.; Došlić, N.; Ivković, J.; Wang, Y. H.; Mališ, P.; Wan, P. *Chem. - Eur. J.* **2012**, *18*, 10617−10623.
(31) Brousmiche, D.; Xu, M.; Lukeman, M.; Wan, P. *J. Am. Chem. Soc.* **2003**, *125*, 12961−12970.
(32) Colloredo-Mels, S.; Doria, F.; Verga, D.; Freccero, M. *J. Org. Chem.* **2006**, *71*, 3889−3895.
(33) Di Antonio, M.; Doria, F.; Mella, M.; Merli, D.; Profumo, A.; Freccero, M. *J. Org. Chem.* **2007**, *72*, 8354−8360.
(34) Verga, D.; Nadai, M.; Doria, F.; Percivalle, C.; Di Antonio, M.; Palumbo, M.; Richter, S. N.; Freccero, M. *J. Am. Chem. Soc.* **2010**, *132*, 14625−14637.
(35) Doria, F.; Richter, S. N.; Nadai, M.; Colloredo-Mels, S.; Mella, M.; Palumbo, M.; Freccero, M. *J. Med. Chem.* **2007**, *50*, 6570−6579.
(36) Nadai, M.; Doria, F.; Di Antonio, M.; Sattin, G.; Germani, L.; Percivalle, C.; Palumbo, M.; Richter, S. N.; Freccero, M. *Biochimie* **2011**, *93*, 1328−1340.
(37) Doria, F.; Nadai, M.; Folini, M.; Di Antonio, M.; Germani, L.; Percivalle, C.; Sissi, C.; Zaffaroni, N.; Alcaro, S.; Artese, A.; Richter, S. N.; Freccero, M. *Org. Biomol. Chem.* **2012**, *10*, 2798−2806.
(38) Doria, F.; Nadai, M.; Folini, M.; Scalabrin, M.; Germani, L.; Sattin, G.; Mella, M.; Palumbo, M.; Zaffaroni, N.; Fabris, D.; Freccero, M.; Richter, S. N. *Chem. - Eur. J.* **2013**, *19*, 78−81.
(39) Stedman, E. *J. Chem. Soc.* **1927**, 1902−1906.
(40) See http://sdbs.db.aist.go.jp/sdbs/cgi-bin/direct_frame_disp.cgi?sdbsno=1680.
(41) Pines, E. In *The Chemistry of Phenols*; Rappoport, Z., Ed. Wiley: New York, 2003.
(42) Ireland, J. F.; Wyatt, P. A. H. *Adv. Phys. Org. Chem.* **1976**, *12*, 131−221.
(43) Arnaut, L. G.; Formosinho, S. J. *J. Photochem. Photobiol., A* **1993**, *75*, 1−20.
(44) Klöpffer, W. *Adv. Photochem.* **1977**, *10*, 311−358.
(45) Formosinho, S. J.; Arnaut, L. G. *J. Photochem. Photobiol., A* **1993**, *75*, 21−48.
(46) Ormson, S. M.; Brown, R. G. *Prog. React. Kinet.* **1994**, *19*, 45−211.
(47) Le Gourrierec, D.; Ormson, S. M.; Brown, R. G. *Prog. React. Kinet.* **1994**, *19*, 211−275.
(48) Montalti, M.; Credi, A.; Prodi, L.; Gandolfi, M. T. *Handbook of Photochemistry*; CRC Taylor and Francis: Boca Raton, 2006.
(49) Tolbert, L. M.; Solntsev, K. M. *Acc. Chem. Res.* **2002**, *35*, 19−27.
(50) Agmon, N. *J. Phys. Chem. A* **2005**, *109*, 13−35.
(51) Gampp, H.; Maeder, M.; Meyer, C. J.; Zuberbühler, A. D. *Talanta* **1985**, *32*, 95−101.
(52) Gampp, H.; Maeder, M.; Meyer, C. J.; Zuberbühler, A. D. *Talanta* **1985**, *32*, 257−264.
(53) Gampp, H.; Maeder, M.; Meyer, C. J.; Zuberbühler, A. D. *Talanta* **1985**, *32*, 1133−1139.
(54) Brown, W.; Iverson, B.; Anslyn, E.; Foote, C. *Organic Chemistry*; Cengage Learning: Belmont, 2014.
(55) Kanamori, D.; Furukawa, A.; Okamura, T.-A.; Yamamoto, H.; Ueyama, N. *Org. Biomol. Chem.* **2005**, *3*, 1453−1459.
(56) Weinert, E. E.; Dondi, R.; Colloredo-Melz, S.; Frankenfield, K. N.; Mitchell, C. H.; Freccero, M.; Rokita, S. E. *J. Am. Chem. Soc.* **2006**, *128*, 11940−11947.
(57) Shikhmamedbekova, A. Z.; Bairamov, G. B. *Katalit. Prevrashch. Kislorod. i Serosoderzh. Organ. Soedin., Baku* **1983**, 74−78.
(58) Liu, Q.; Rovis, T. *J. Am. Chem. Soc.* **2006**, *128*, 2552−2553.
(59) Lee, J.; Robinson, G. W.; Webb, S. P.; Philips, L. A.; Clark, J. H. *J. Am. Chem. Soc.* **1986**, *108*, 6538−6542.
(60) Robinson, G. W. *J. Phys. Chem.* **1991**, *95*, 10386−10391.
(61) Tolbert, L. M.; Haubrich, J. E. *J. Am. Chem. Soc.* **1994**, *116*, 10593−10600.
(62) Solntsev, K. M.; Huppert, D.; Agmon, N.; Tolbert, L. M. *J. Phys. Chem. A* **2000**, *104*, 4658−4669.
(63) Wan, P.; Chak, B. *J. Chem. Soc., Perkin Trans. 2* **1986**, *11*, 1751.
(64) Basarić, N.; Cindro, N.; Bobinac, D.; Mlinarić-Majerski, K.; Uzelac, L.; Kralj, M.; Wan, P. *Photochem. Photobiol. Sci.* **2011**, *10*, 1910−1925.
(65) Basarić, N.; Cindro, N.; Bobinac, D.; Uzelac, L.; Mlinarić-Majerski, K.; Kralj, M.; Wan, P. *Photochem. Photobiol. Sci.* **2012**, *11*, 381−396.
(66) Veljković, J.; Uzelac, L.; Molčanov, K.; Mlinarić-Majerski, K.; Wan, P.; Basarić, N. *J. Org. Chem.* **2012**, *77*, 4596−4610.
(67) Van de Water, R. W.; Pettus, T. R. R. *Tetrahedron* **2002**, *58*, 5367−5405.
(68) Cao, S.; Christiansen, R.; Peng, X. *Chem. - Eur. J.* **2013**, *19*, 9050−9058.
(69) Krohn, K.; Rieger, H.; Khanbabaee, K. *Chem. Ber.* **1989**, *122*, 2323−2330.
(70) Goldstein, S.; Rabani, J. *J. Photochem. Photobiol., A* **2008**, *193*, 50−55.

DOI: 10.1021/acs.joc.5b01991
J. Org. Chem. 2015, 80, 10817−10828

(71) Kuhn, H. J.; Braslavsky, S. E.; Schmidt, R. *Pure Appl. Chem.* **2004**, *76*, 2105−2146.
(72) Mitchell, R. H.; Bohne, C.; Wang, Y.; Bandyopadhyay, S.; Wozniak, C. B. *J. Org. Chem.* **2006**, *71*, 327−336.
(73) Chiang, Y.; Kresge, A. J.; Zhu, Y. *J. Am. Chem. Soc.* **2000**, *122*, 9854−9855.
(74) Chiang, Y.; Kresge, A. J.; Zhu, Y. *J. Am. Chem. Soc.* **2001**, *123*, 8089−8094.
(75) Chiang, Y.; Kresge, A. J.; Zhu, Y. *J. Am. Chem. Soc.* **2002**, *124*, 717−722.
(76) Richard, J. P.; Toteva, M. M.; Crugeiras, J. *J. Am. Chem. Soc.* **2000**, *122*, 1664−1674.
(77) Toteva, M. M.; Richard, J. P. *Adv. Phys. Org. Chem.* **2011**, *45*, 39−91.
(78) Ottosson, H. *Nat. Chem.* **2012**, *4*, 969−970.
(79) Rosenberg, M.; Dahlstrand, C.; Kilså, K.; Ottosson, H. *Chem. Rev.* **2014**, *114*, 5379−5425.
(80) Wang, H.; Wahi, M. S.; Rokita, S. E. *Angew. Chem., Int. Ed.* **2008**, *47*, 1291−1293.
(81) Wang, H.; Rokita, S. E. *Angew. Chem., Int. Ed.* **2010**, *49*, 5957−5960.
(82) Rossiter, C. S.; Modica, E.; Kumar, D.; Rokita, S. E. *Chem. Commun.* **2011**, *47*, 1476−1478.
(83) Houben, J., Weyl, T., Eds. *Methoden der Organische Chemie*; Georg Thieme Verlag: Stuttgart, 1957; Vol. *11/1*.
(84) Tamilselvi, A.; Mugesh, G. *Inorg. Chem.* **2011**, *50*, 749−756.
(85) Škalamera, Đ.; Mlinarić-Majerski, K.; Martin-Kleiner, I.; Kralj, M.; Wan, P.; Basarić, N. *J. Org. Chem.* **2014**, *79*, 4390−4397.
(86) Liao, Y.; Bohne, C. *J. Phys. Chem.* **1996**, *100*, 734−743.

DOI: 10.1021/acs.joc.5b01991
J. Org. Chem. 2015, 80, 10817−10828